Pflügers Arch - Eur J Physiol (2001) 441:787–795
DOI 10.1007/s004240000476

ORIGINAL ARTICLE

Meng-Ru Shen · Cheng-Yang Chou · J. Clive Ellory

Swelling-activated taurine and K^+ transport in human cervical cancer cells: association with cell cycle progression

Received: 24 August 2000 / Received after revision: 11 October 2000 / Accepted: 16 October 2000 / Published online: 16 December 2000

Abstract The aim of this study was to investigate swelling-activated taurine and K^+ transport in human cervical cancer cells under various culture conditions, testing the hypothesis that the progression of cell cycle was accompanied by differential activities of swelling-activated transport pathways. Aphidicolin, an inhibitor of deoxyribonucleic acid (DNA) synthesis, was used to synchronize the cell cycle. The distribution of cell cycle stage was determined by fluorescence-activated cell sorting (FACS). Hypotonicity activated taurine efflux, which was sensitive to tamoxifen and 5-nitro-2-(3-phenylpropylamino) benzoic acid (NPPB). Cell swelling also induced both Cl^--dependent and -independent K^+ ($^{86}Rb^+$) efflux, presumably mediated by KCl cotransport (KCC) and Ca^{2+}-activated K^+ channels, respectively. Cell cycle arrest in G0/G1 was accompanied by a remarkable decrease in the rate constant for swelling-activated taurine efflux, from 0.20±0.007 to 0.026±0.002 min^{-1} (n=6). The activity of swelling-activated taurine efflux recovered progressively on re-entry into the cell cycle. After removal of aphidicolin and culture with 10% fetal calf serum for 10 h, the rate constant increased significantly from 0.026±0.002 to 0.093±0.002 min^{-1} (n=6). After 24 h release from aphidicolin, the efflux rate constant had increased further to 0.195±0.006 min^{-1} (n=6), a value not significantly different from that in normally proliferating cells. The differential activities of swelling-activated taurine transport matched well with our previous study showing a volume-sensitive anion channel associated with cell cycle progression. In contrast to the differential activities of swelling-activated taurine transport, swelling-activated K^+ ($^{86}Rb^+$) transport was independent of the progression of cell cycle. Most importantly, pharmacological blockade of swelling-activated taurine efflux by tamoxifen or NPPB caused proliferating cervical cancer cells to arrest in G0/G1, suggesting that the activity of this efflux was associated with G1/S checkpoint progression. This study provides new and important information on the functional significance of swelling-activated transport system in the regulation of cell cycle clock of human cervical cancer cells.

Keywords Cervical cancer · Cell cycle · Taurine · KCl cotransport · K^+ channel

M.-R. Shen · J.C. Ellory (✉)
University Laboratory of Physiology, Parks Road,
Oxford OX1 3PT, United Kingdom
e-mail: clive.ellory@physiol.ox.ac.uk
Tel.: +44-1865-272436, Fax: +44-1865-272488

M.-R. Shen · C.-Y. Chou
Department of Obstetrics and Gynaecology, College of Medicine,
National Cheng Kung University, Tainan 704, Taiwan

Introduction

Most epithelial cells defend their volume against hypotonic stress by losing solutes together with osmotically obligated water, a process termed regulatory volume decrease (RVD). The principal solutes lost in RVD are K^+, Cl^- and a group of largely uncharged organic solutes known as organic osmolytes. These organic osmolytes are present at high intracellular concentrations in some types of cells and may play a central role in cellular osmoregulation and cytoprotection [14]. Taurine is a major representative of these organic osmolytes [11, 14]. In response to hypotonic stress, K^+ and Cl^- can cross the membrane either via separate K^+ and anion channels, or via the electroneutral KCl cotransporter (KCC) [11]. Much attention has been focused on the volume-sensitive anion channel, since it shows a broad sensitivity for different anions and organic osmolytes [23]. In addition to volume regulation and osmolyte transport, the volume-sensitive anion channel participates in important physiological processes, such as metabolic events, hormone release, cell proliferation, differentiation and cell death [16, 22].

Cervical cancer is the most common gynaecological malignancy world-wide [25]. This disease is associated strongly with infection by oncogenic types of human papillomavirus (HPV), but only a small fraction of patients develop cancer, indicating that other factors con-

tribute to the progression to cervical cancer [41]. Despite intensive study, the aetiology and tumour biology of this disease are still largely unknown, and the membrane transport properties of human cervical epithelial cells have received little attention. We have demonstrated previously that K^+, Cl^- and organic osmolyte efflux are upregulated strongly in the malignant transformation of human cervical epithelial cells [4, 5, 29, 32]. In addition, the volume-sensitive ion channel and cotransport systems work synergistically for volume regulation in human cervical cancer cells [32]. Alterations in osmosensing signalling pathways are also apparent during the process of human cervical carcinogenesis [6, 30].

Several studies have shown that differential expression of K^+ channels and concomitant changes in membrane potential are critical for cell cycle checkpoints (reviewed in [39]). Cell volume undergoes a significant change during the cell cycle progression [1], which perturbs cell volume homeostasis and should be counterbalanced by RVD. Activation of volume-sensitive transport systems is therefore proposed to be a necessary step for volume regulation during the cell cycle progression. However, very little is known about the association between the cell cycle and volume-sensitive ion transport.

Our very recent study has shown the differential activities of volume-sensitive anion channel during the cell cycle progression of human cervical cancer SiHa cells [33]. We did not know, however, whether taurine was released via volume-sensitive anion channel during RVD in these cells. In addition, we were interested in the activity of swelling-activated K^+ transport during the cell cycle. The aim of the present study was therefore to investigate swelling-activated taurine and K^+ transport in human cervical cancer SiHa cells under various culture conditions, testing the hypothesis that progression of the cell cycle is accompanied by differential activities of swelling-activated transport pathways. The results demonstrated that the cell cycle progression was accompanied by differential activities of swelling-activated taurine transport, which matched well with those of volume-sensitive anion channel.

Materials and methods

Cell culture

SiHa cells, a cervical cancer cell line, were obtained from the American Type Culture Collection (Rockville, Md., USA) and maintained at 37 °C in a CO_2-air (5%-95%) atmosphere and cultured in Dulbecco's modified Eagle's medium (DMEM; Gibco, Grand Island, N.Y., USA) supplemented with 10% fetal calf serum (FCS; Gibco), 80 IU/ml penicillin and 80 µg/ml streptomycin (Sigma-Aldrich, Dorset, England).

Chemicals and solutions

All chemicals were obtained from Sigma-Aldrich. The osmolarity of solutions was measured using a vapour pressure osmometer (Wescor 5500, Schlag Instruments, Gladbach, Germany). The isotonic solution contained (in mM): NaCl 100, KCl 5, $MgCl_2$ 1, $CaCl_2$ 1.5, glucose 10, 4-(2-hydroxyethyl)-1-piperazineethanesulphonic acid (HEPES) 10 and mannitol 80, titrated to pH 7.4 with NaOH (300±3 mosm/l). The hypotonic solution was the same as the isotonic solution except for the omission of mannitol, resulting in 27% hypotonicity (220±3 mosm/l). The solvent for various chemicals was dimethylsulphoxide (DMSO). The final DMSO concentration in experiments of flux and cell proliferation was less than 0.05%; this had no effect on measured fluxes or cell proliferation.

Cell cycle synchronization

For experiments on cell synchronization, SiHa cells were seeded initially at a concentration of 1×10^4 cells/cm^2 in six-well culture plates and grown to 60–80% confluence to obtain cultures in the logarithmic growth phase. In experiments on serum starvation, cell cultures were washed 3 times with DMEM and then cultured in DMEM supplemented with 0.1% FCS. For chemical synchronization, cultures were growth-arrested by serum starvation for 2 days and then treated with 10 µM aphidicolin for 12 h. Aphidicolin, an inhibitor of deoxyribonucleic acid (DNA) synthesis, can prevent cells in the G0/G1 phase from entering the DNA synthetic period [17]. Identically treated cultures grown in parallel were harvested for fluorescence-activated cell sorting (FACS) and flux experiments at the indicated times. Synchronization experiments were repeated at least 3 times. In experiments on cell proliferation, cell counts were performed with the aid of a haemocytometer using trypan blue exclusion (0.08%) to monitor cell viability [40].

Determination of cell cycle stage by FACS

Cell DNA content was determined by staining cells with propidium iodide and measuring fluorescence (FACScan, Becton-Dickinson, Rutherford, N.J., USA). Cervical cancer SiHa cells were harvested by trypsinization and fixed in cool 70% ethanol for 6 h. Subsequently, the fixed cells were incubated in a solution containing 1 mg/ml RNase and 20 µg/ml propidium iodide for at least 1 h. For each cell population, 10,000 cells were analysed by FACS and the proportions in G0/G1, S and G2/M phases estimated using the Modfit cell cycle analysis program (v. 2.0, Verity Software House). The percentage of cells in a specific phase of the cell cycle was determined with a propidium iodide DNA staining technique. Cells were classified in G0/G1, G2/M and S phase depending on the intensity of the fluorescent peaks [18]. FACS measurements were performed in four independent experiments on synchronization or unsynchronization.

Functional [^{3}H]taurine efflux assays

[^{3}H]taurine efflux experiments were carried out at room temperature as described in detail elsewhere [10]. In brief, SiHa cells, grown on six-well plates, were pre-incubated with isotonic culture medium loaded with 1 µCi/ml [^{3}H]taurine for 2 h at 37 °C. After pre-incubation, the loading medium was aspirated and cells washed rapidly 7 times with phosphate-buffered saline. After washing, appropriate efflux medium was added to the cells. A 1-ml aliquot of efflux medium was replaced at indicated time intervals and saved for counting. Release of [^{3}H]taurine from preloaded cells was measured in the efflux medium at indicated time intervals within a 20 min duration. Cells were finally lysed with 0.5 M NaOH to release the remaining [^{3}H]taurine. The radioactivity present in the efflux samples and in cell lysates was then determined by liquid scintillation counting. [^{3}H]taurine efflux rate constants were estimated from the negative slope of the graph of $\ln[X_{i(t)}/X_{i(t=0)}]$ vs. time (t), where $X_{i(t=0)}$ denotes the total amount of [^{3}H]taurine inside the cells at the beginning of the efflux time course and $X_{i(t)}$ the amount of [^{3}H]taurine inside the cells at time t. In some experiments, taurine release was expressed as fractional taurine efflux, which was defined as the [^{3}H]taurine release in

each fraction as a percentage of the total [^{3}H]taurine present in the cells at the indicated time.

Functional $^{86}Rb^+$ efflux assays

$^{86}Rb^+$ is a valid congener for K^+ transport and, therefore, $^{86}Rb^+$ efflux assays were used to study the activity of K^+ transport in various experimental conditions. Efflux experiments were carried out as described in detail elsewhere [32]. In brief, unidirectional K^+ efflux was measured in cells grown on six-well plates using $^{86}Rb^+$ as tracer. Cells were pre-incubated with isotonic culture medium loaded with 2 µCi/ml $^{86}Rb^+$ for 2 h at 37 °C. After preincubation, the loading medium was aspirated and cells were washed rapidly 7 times with phosphate-buffered saline. After washing, the appropriate efflux medium (containing 0.1 mM ouabain and 0.01 mM bumetanide to inhibit the Na^+-K^+ pump and the $Na^+K^+2Cl^-$ cotransporter, respectively) was added to the cells. Release of $^{86}Rb^+$ from preloaded cells was measured in the efflux medium at indicated time intervals within a 20 min duration. Cells were finally lysed with 50% trichloroacetic acid to release remaining cellular $^{86}Rb^+$. $^{86}Rb^+$ efflux rate constants were estimated from the negative slope of the graph of $\ln[X_{i(t)}/X_{i(t=0)}]$ vs. t, where $X_{i(t=0)}$ denotes the total amount of $^{86}Rb^+$ inside the cells at the beginning of the efflux time course and $X_{i(t)}$ the amount of $^{86}Rb^+$ inside the cells at the time t. The hypotonicity-induced efflux was the difference between the effluxes in the isotonic media and hypotonic media.

KCl cotransport was taken as the Cl^--dependent K^+ ($^{86}Rb^+$) flux in the presence of 0.01 mM bumetanide [32]. To study the activity of KCl cotransport, the Cl^- dependence of K^+ ($^{86}Rb^+$) efflux was examined by substituting methylsulphate ($CH_3OSO_3^-$) for Cl^- in the efflux medium. The Cl^--dependent K^+ ($^{86}Rb^+$) flux was defined as the efflux difference between Cl^- and $CH_3OSO_3^-$ media.

Data analysis

Data are presented as mean±SEM. ANOVA, Student's paired or unpaired *t*-tests were used as appropriate for statistical analyses. Differences between values were considered significant when $P<0.05$.

Results

Distribution of cell cycle stages

Cell DNA content was measured by FACS to determine the cell cycle distribution under various culture conditions (Fig. 1). In the presence of 10% FCS for 48 h, 56±0.8%, 7.0±0.6% and 37±1.0% of cells were in G0/G1, S and G2/M stages respectively (Fig. 1A, control group, n=4). To synchronize the cell cycle, cervical cancer SiHa cells were initially deprived of FCS for 48 h and subsequently incubated with 10 µM aphidicolin for 12 h. This treatment significantly increased the percentage of cells arrested in G0/G1 stage (Fig. 1B, n=4, 89±1.0% vs. 56±0.8% of control groups, $P<0.01$). Removal of aphidicolin triggered rapid re-entry into the cell cycle. By 10 h after removal of aphidicolin, only 41±1% of cells were in the G0/G1 stage, whereas 20±1% and 39±1.2% of cells had reached the S and G2/M stages respectively (Fig. 1C, n=4). The cell cycle stage had a similar distribution with control groups after 24 h release from aphidicolin (Fig. 1D). Thus, aphidicolin effectively and reversibly arrested cervical cancer cells in the G0/G1 stage.

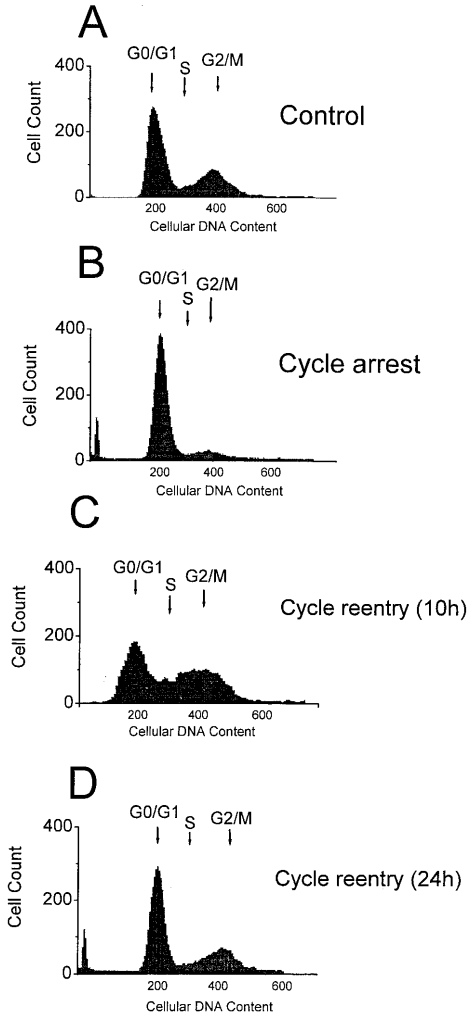

Fig. 1A–D Representative results of fluorescence-activated cell sorting (FACS) measurements to determine cell cycle stages of cervical cancer SiHa cells under various culture conditions. **A** *Control*: culture in the presence of 10% fetal calf serum (FCS) for 48 h. **B** *Cycle arrest*: cultures growth-arrested by serum starvation for 2 days followed by 10 µM aphidicolin for 12 h. **C, D** Cycle re-entry: Release of aphidicolin and culture with 10% FCS for 10 h (**C**) and 24 h (**D**) (*G0/G1*, *S*, *G2/M* cell cycle phases, *DNA* deoxyribonucleic acid)

Hypotonicity activated NPPB- and tamoxifen-sensitive taurine efflux

Figure 2A shows the time course of taurine efflux from SiHa cells exposed to isotonic and hypotonic media. Basal taurine efflux of SiHa cells was low and stable in the isotonic solution. The swelling-activated taurine efflux was reversible when isotonicity of the extracellular medium was restored (Fig. 2A). Exposure to the hypotonic solution markedly increased the taurine efflux rate constant from 0.0095±0.002 min^{-1} to 0.20±0.007 min^{-1} (Fig. 2B, n=6). The swelling-activated taurine efflux was inhibited significantly by 50 µM 5-nitro-2-(3-phenylpropylamino) benzoic acid (NPPB) and 5 µM tamoxifen, two well-known Cl^- channel blockers (about 60% and 70% inhibition of hypotonicity-activated taurine efflux,

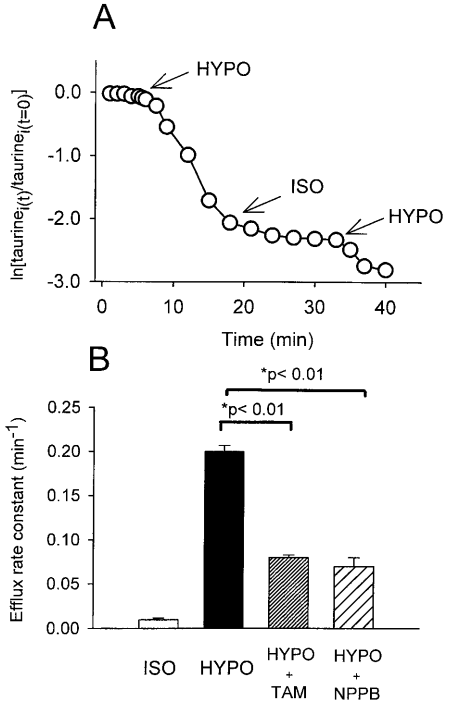

Fig. 2A, B Hypotonicity activates taurine efflux that is sensitive to 5-nitro-2-(3-phenylpropylamino) benzoic acid (*NPPB*) and tamoxifen (*TAM*). **A** Time course of taurine efflux from SiHa cells exposed to isotonic and hypotonic media. Graph shows logarithm (*ln*) of the fraction of the original intracellular [^{3}H]taurine remaining as a function of time. At times marked *HYPO*, efflux medium changed from 300 to 220 mosm/l. At the point marked *ISO*, efflux medium restored to 300 mosm/l. Means, *n*=6. **B** Swelling-activated [^{3}H]taurine efflux is sensitive to 5 μM TAM and 50 μM NPPB. Means±SEM, *n*=6. **P*<0.01 between groups (unpaired *t*-test)

respectively). This potency is close to that for their inhibitory effects on the volume-sensitive Cl^- channel of cervical cancer cells [29, 31].

Hypotonicity activates K^+ ($^{86}Rb^+$) efflux that is mediated by K^+ channels and KCl cotransport

Figure 3A shows the time course of K^+ ($^{86}Rb^+$) efflux from SiHa cells exposed to isotonic and hypotonic media. The K^+ ($^{86}Rb^+$) efflux was low and stable under isotonic conditions. Exposure to the hypotonic solution markedly increased the K^+ ($^{86}Rb^+$) efflux rate constant from 0.006±0.0006 to 0.017±0.001 min^{-1} (Fig. 3B, *n*=6). The swelling-activated K^+ ($^{86}Rb^+$) efflux was reversible when the extracellular medium returned to the isotonic solution (Fig. 3A).

KCl cotransport was taken as the Cl^--dependent K^+ ($^{86}Rb^+$) flux in the presence of 0.01 mM bumetanide. Subsequently, the Cl^- dependence of K^+ ($^{86}Rb^+$) efflux

Fig. 3A–D Hypotonicity activates K^+ ($^{86}Rb^+$) efflux that is mediated by K^+ channels and KCl cotransport. **A** Time course of K^+ ($^{86}Rb^+$) efflux from SiHa cells exposed to isotonic and hypotonic media. Graph shows logarithm of fraction of original intracellular K^+ ($^{86}Rb^+$) remaining as a function of time. Means, *n*=6. **B** K^+ ($^{86}Rb^+$) efflux rate in isotonic (300 mosm/l) and hypotonic (220 mosm/l) conditions. SiHa cells were incubated with 2 μCi/ml $^{86}Rb^+$ at 37 °C for 2 h and then efflux assays run as described in Materials and methods. Means±SEM, *n*=6. **C** Time course of K^+ ($^{86}Rb^+$) efflux from SiHa cells exposed to isotonic and hypotonic media. *HYPO*: efflux medium changed from 300 to 220 mosm/l medium containing various inhibitors {10 μM [(dihydroindenyl)oxy]alkanoic acid (*DIOA*), 10 μM clotrimazole, 10 μM DIOA plus 10 μM clotrimazole, or 300 μM NPPB}. Means±SEM, *n*=6. **D** K^+ ($^{86}Rb^+$) efflux rate under hypotonic solution (*Control*), isotonic solution (*ISO*) or hypotonic solution containing various inhibitors. Means±SEM *n*=6. **P*<0.05 vs. control, unpaired *t*-test

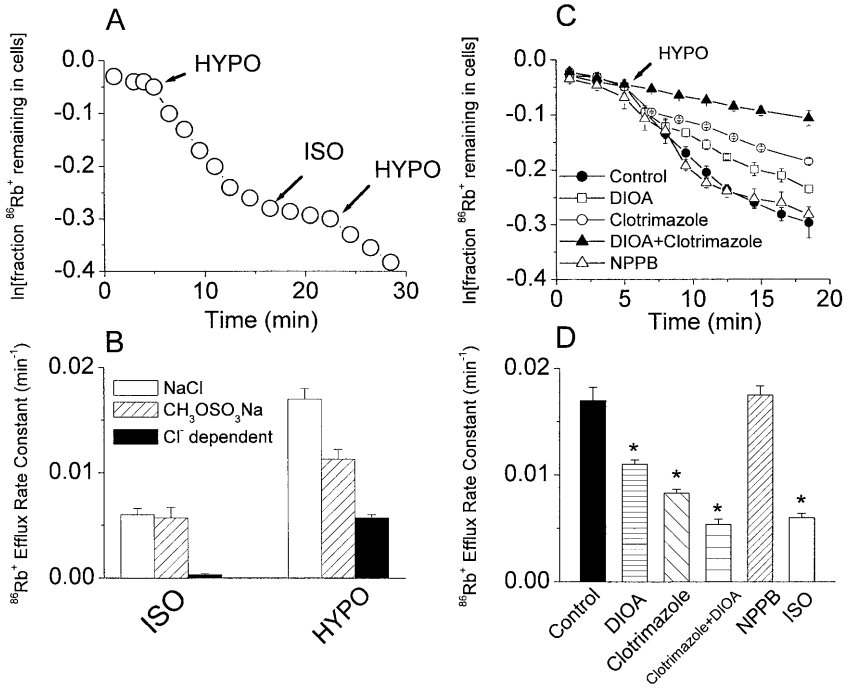

was examined by substituting $CH_3OSO_3^-$ for Cl^- in the efflux medium. The Cl^--dependent K^+ ($^{86}Rb^+$) flux was defined as the difference in efflux between Cl^- and $CH_3OSO_3^-$ media. In isotonic medium, the Cl^--dependent K^+ ($^{86}Rb^+$) efflux was very low, being 0–5% of total K^+ ($^{86}Rb^+$) efflux (Fig. 3B). Hypotonic stress stimulated the Cl^--dependent K^+ ($^{86}Rb^+$) efflux markedly, which then constituted 33% of total K^+ ($^{86}Rb^+$) efflux in the hypotonic solution (Fig. 3B). In addition, the swelling-activated K^+ ($^{86}Rb^+$) efflux was sensitive to [(dihydroindenyl)oxy]alkanoic acid (DIOA) and clotrimazole, inhibitors of KCC and the Ca^{2+}-activated K^+ channel, respectively (Fig. 3C and D). However, swelling-activated K^+ ($^{86}Rb^+$) efflux was refractory to NPPB, a Cl^- channel inhibitor, at concentrations up to 300 μM (Fig. 3C and D). DIOA (10 μM) and clotrimazole (10 μM) inhibited 30–40% and 50–60% of total hypotonic K^+ ($^{86}Rb^+$) transport, respectively. Furthermore, 10 μM DIOA plus 10 μM clotrimazole completely abolished the swelling-activated K^+ ($^{86}Rb^+$) efflux (Fig. 3C and D). Together with the results from Cl^- replacement, this indicates that both K^+ channels and KCl cotransport work synergistically in mediating swelling-activated K^+ transport.

Influence of Ca^{2+} on the swelling-activated K^+ ($^{86}Rb^+$) efflux

The above results demonstrated that the swelling-activated K^+ ($^{86}Rb^+$) efflux is sensitive to clotrimazole, a fairly specific inhibitor of Ca^{2+}-activated K^+ channel [34]. Accordingly, we investigated the influence of Ca^{2+} on the swelling-activated K^+ ($^{86}Rb^+$) efflux (Fig. 4). In the absence of external Ca^{2+} ($[Ca^{2+}]_o$), 27±2% and 30±3% of swelling-activated K^+ ($^{86}Rb^+$) efflux was decreased in Cl^- and $CH_3OSO_3^-$ media, respectively. The reduction in K^+ ($^{86}Rb^+$) efflux was not significantly different between Cl^- and $CH_3OSO_3^-$ flux media, indicating that the Cl^- dependent K^+ ($^{86}Rb^+$) efflux (KCl cotransport) is insensitive to $[Ca^{2+}]_o$. In the Ca^{2+}-depleted cells, treatment with 1 μM thapsigargin in Ca^{2+}-free medium decreased further the already reduced swelling-activated K^+ ($^{86}Rb^+$) efflux to 50–60% of that in the Cl^- efflux medium. Moreover, it was completely inhibited in the $CH_3OSO_3^-$ medium. Since K^+ transport in $CH_3OSO_3^-$ medium is via K^+ channels, this result indicates the activation of K^+ channels by cell swelling depends on both extracellular Ca^{2+} entry and intracellular stores. To buffer free Ca^{2+} further, SiHa cells were pre-incubated with 50 μM 1,2-bis(2-aminophenoxy)ethane-*N*,*N*,*N*′,*N*′-tetraacetic acid, tetrakis(acetoxymethyl)ester (BAPTA-AM) for 30 min and efflux measured in the Ca^{2+}-free medium. This treatment abolished 80% of swelling-activated K^+ ($^{86}Rb^+$) transport in the Cl^- efflux medium. In the $CH_3OSO_3^-$ efflux medium, this treatment not only completely abolished swelling-activated K^+ ($^{86}Rb^+$) efflux, but also inhibited 45±3% of basal K^+ ($^{86}Rb^+$) efflux (Fig. 4). This suggests the basal K^+ transport in the isotonic solution depends partly on Ca^{2+}.

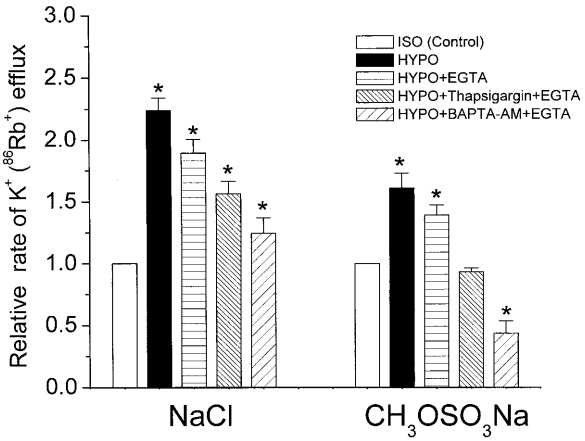

Fig. 4 Influence of Ca^{2+} on swelling-activated K^+ ($^{86}Rb^+$) efflux. K^+ transport in Cl^- or $CH_3OSO_3^-$ efflux medium. The isotonic K^+ ($^{86}Rb^+$) efflux rate was used as control and other rates expressed relative to it. *ISO*: 300 mosm/l; *HYPO*: 220 mosm/l; *HYPO+EGTA*: Ca^{2+}-free hypotonic solution with 1.5 mM ethyleneglycol-bis(β-aminoethylether)-*N*,*N*,*N*′,*N*′-tetraacetic acid; *HYPO+Thapsigargin+EGTA*: SiHa cells pre-incubated with 1 μM thapsigargin for 30 min and efflux measured in Ca^{2+}-free medium containing 1.5 mM EGTA; *HYPO+BAPTA-AM+EGTA*: SiHa cells pre-incubated with 50 μM 1,2-bis(2-aminophenoxy)ethane-*N*,*N*,*N*′,*N*′-tetraacetic acid, tetrakis(acetoxymethyl)ester for 30 min and efflux measured in Ca^{2+}-free medium containing 1.5 mM EGTA. Means±SEM, n=6. *P<0.05 vs. control, unpaired t-test

Down-regulation of taurine efflux in cells arrested in G0/G1 stage

In the next series of experiments, we compared swelling-activated taurine efflux in synchronized and unsynchronized cells (Fig. 5). Cervical cancer cells presented similar time courses for swelling-activated taurine efflux under various culture conditions. After an initial 1- to 1.5-min lag, the stimulatory effect on taurine efflux reached a maximum within 2 min and then gradually declined in the continuing presence of the hypotonic stress (Fig. 5A). The unsynchronized cells had a small basal taurine efflux rate constant in the isotonic medium, averaging 0.0095±0.0002 min^{-1} (Fig. 5B, n=8, control group). For cervical cancer cells synchronized in G0/G1 phase, the background taurine efflux rate constant was 0.0087±0.0009 min^{-1} (n=6). There was no significant difference in background isotonic taurine efflux between these two groups of cells.

For unsynchronized cells growing in 10% FCS, exposure to hypotonicity activated rapid taurine efflux with a rate constant of 0.20±0.007 min^{-1} (Fig. 5B). Volume-activated taurine efflux was still present in arrested cells, but the efflux rate decreased significantly to 0.026± 0.002 min^{-1} (P<0.001; Fig. 5B). This indicates that the arrest of the cell cycle in G0/G1 is accompanied by a remarkable decrease in the activity of swelling-activated taurine efflux.

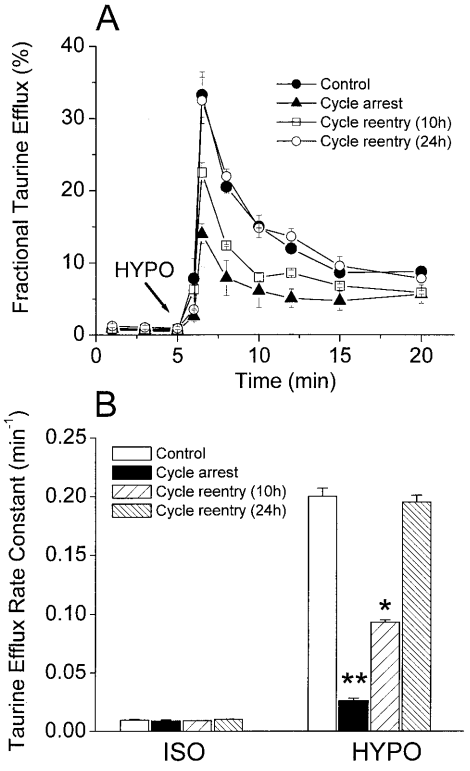

Fig. 5A, B Differential activities of swelling-activated taurine efflux during cell cycle progression. **A** Time course of fractional [^{3}H]taurine release for SiHa cells under various culture conditions. Means±SEM, *n*=6. **B** [^{3}H]taurine efflux rate under various culture conditions. Means±SEM, *n*=6. *ISO*: 300 mosm/l; *HYPO*: 220 mosm/l. **P*<0.01; ***P*<0.001 vs. control, unpaired *t*-test

Recovery of taurine efflux after cell cycle re-entry

We subsequently investigated whether the activity of swelling-activated taurine efflux recovered with re-entry into the cell cycle. After removal of aphidicolin and culture with 10% FCS for 10 h, the swelling-activated taurine efflux rate constant increased significantly from 0.026±0.002 to 0.093±0.002 min^{-1} (Fig. 5, *n*=6). After 24 h release from aphidicolin, the efflux rate had increased further to 0.195±0.006 min^{-1} (*n*=6), which was not significantly different from that of normally proliferating cells. Therefore, increasing activity of swelling-activated taurine efflux accompanies re-entry into the cell cycle.

We also investigated the acute effect of aphidicolin on the swelling-activated taurine efflux to rule out the possibility that the down-regulation of taurine efflux in cells arrested in the G0/G1 stage is caused by a non-specific effect of aphidicolin. Pre-incubated for 30 min at 37 °C, aphidicolin up to 20 µM had no effect on the volume-sensitive taurine efflux (data not shown). This supports the idea that differential activities of the swelling-activated taurine efflux are a specific consequence of the progression of the cell cycle.

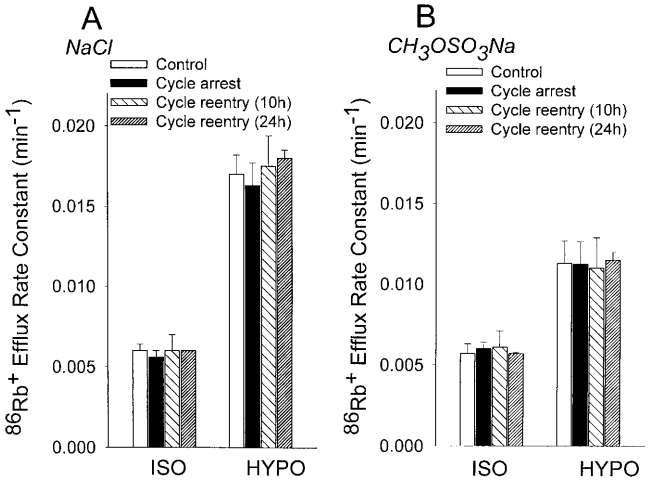

Fig. 6A, B Swelling-activated K^+ ($^{86}Rb^+$) efflux is independent of the progression of cell cycle. **A** K^+ ($^{86}Rb^+$) transport in Cl^- efflux medium for SiHa cells under various culture conditions. **B** K^+ ($^{86}Rb^+$) transport in $CH_3OSO_3^-$ efflux medium for SiHa cells under various culture conditions. Means±SEM, *n*=6. *ISO*: 300 mosm/l; *HYPO*: 220 mosm/l

The swelling-activated K^+ ($^{86}Rb^+$) efflux is independent of the progression of the cell cycle

We also investigated the possible change of swelling-activated K^+ ($^{86}Rb^+$) efflux during cell cycle progression (Fig. 6). There was no significant difference in background isotonic K^+ ($^{86}Rb^+$) efflux among various culture conditions. With cell cycle arrest, hypotonic stress increased the K^+ ($^{86}Rb^+$) efflux rate constant to 0.0163± 0.0014 min^{-1}, which is not significantly different from that of the control group (0.0170±0.0012 min^{-1}, *n*=6,). Similar efflux rates were also noted during cell cycle re-entry (0.0175±0.0019 and 0.0180±0.0006 min^{-1} for 10 h and 24 h cell cycle re-entry, respectively). Similar results were obtained when $CH_3OSO_3^-$ substituted for Cl^- in the efflux medium (Fig. 6B). In contrast to the differential activities of taurine transport, the activation of swelling-activated K^+ ($^{86}Rb^+$) efflux is independent of the progression of the cell cycle.

Blockade of swelling-activated taurine efflux arrests proliferating cervical cancer cells in the G0/G1 stage

We finally investigated whether the potent inhibitors of swelling-activated taurine efflux, tamoxifen and NPPB, inhibit the proliferation of cervical cancer cells and, if so, whether the inhibitory effect on cell growth is due to arrest of the cells in the G0/G1 stage. Figure 7A shows the inhibitory effect of tamoxifen and NPPB on cell proliferation. Cervical cancer SiHa cells were seeded initially at the same cell numbers and counted after 2 days incubation with or without inhibitors. Tamoxifen (5 µM), which blocked 60% of swelling-activated taurine efflux, inhibited 65% of cell proliferation. NPPB (50 µM),

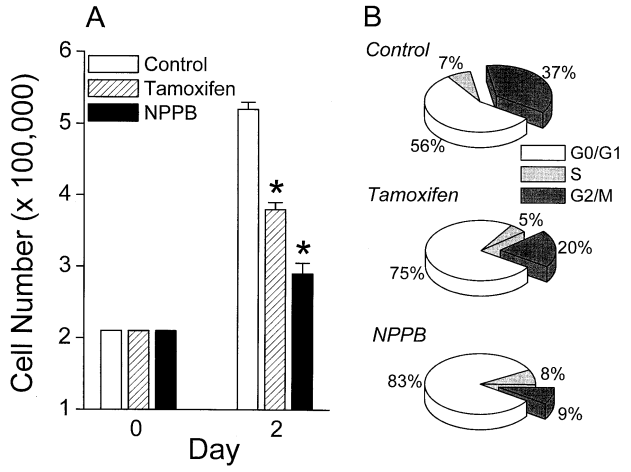

Fig. 7A, B Blockade of swelling-activated taurine efflux by tamoxifen and NPPB arrests proliferating cervical cancer SiHa cells in the G0/G1 phase. **A** Inhibition of the proliferation of cervical cancer cells by 5 μM tamoxifen and 50 μM NPPB. Cell numbers counted initially and recounted after 2 days incubation with or without inhibitors. Means±SEM, n=4. *P<0.01 vs. control (unpaired t-test). **B** Simultaneous FACS measurement for the distribution of cell cycle phases G0/G1, S and G2/M after 2 days incubation with or without inhibitors. Means, n=4

which blocked 70% of taurine efflux, inhibited 73% of cell proliferation. By trypan blue exclusion (0.08%), the cell viability was 93±1%, 91±3% and 89±2% (n=3) for control group, tamoxifen-treated and NPPB-treated cells, respectively. The viability of cells grown in the presence of tamoxifen or NPPB was not different from the control group, suggesting that tamoxifen and NPPB were inhibiting cell growth rather than causing cell death. The simultaneous FACS measurements showed that 75±2% and 83±3% of cervical cancer cells were arrested in the G0/G1 stage by tamoxifen and NPPB, respectively. By contrast, in the absence of inhibitors, only 56±3% of cells were in G0/G1 (Fig. 7B). These results indicate that pharmacological blockade of swelling-activated taurine efflux by tamoxifen or NPPB causes proliferating cervical cancer cells to arrest in G0/G1, suggesting that the activity of this efflux is associated with G1/S checkpoint progression.

Discussion

This study demonstrates a direct correlation between swelling-activated taurine transport and cell cycle progression. What is the functional significance of the differential expressions of swelling-activated taurine transport during cell cycle progression? The most likely possibility is the involvement of swelling-activated organic osmolyte channels in cell volume regulation and metabolism. Proliferating cells usually have higher rates of metabolism, mitosis and migration than cells in growth arrest. Growth, mitosis and migration all perturb cell volume homeostasis. The maintenance of cell volume homeostasis is a fundamental property of mammalian cells, and all cells possess mechanisms for regulating volume during osmotic challenge. Therefore, some beneficial and necessary mechanisms are proposed to be activated in the processes of cellular proliferation and growth. The close linkage of cell volume homeostasis, cell growth and proliferation indicates that swelling-activated organic osmolyte channels play an important role in the processes of the cell cycle clock. Furthermore, during G1/S transition, cells prepare for S entry and are committed to important tasks, including uptake of amino acids, metabolic substrates, materials for synthesis of DNA and proteins and the processing of cell-cycle regulatory signals [39]. Swelling-activated organic osmolyte channels function as a potential transport pathway for metabolic compounds (e.g. amino acids) that are required for cell growth [5, 13]. Moreover, the cell cycle rate might be maximal at a slightly acid intracellular pH since, for example, intracellular alkalinization inhibits proliferation in astrocytes [24]. The swelling-activated organic osmolyte channel may be involved also in pH-regulation and its inhibition may induce cell alkalinization [28]. The activity of the volume-sensitive anion channel in human cervical cancer cells differs during the cell cycle progression [33]. Here we demonstrated that swelling-activated taurine transport and volume-sensitive anion channels might share identical pathways. More importantly, the differential activities of swelling-activated taurine transport matched well with that of the volume-sensitive anion channel during the progression of the cell cycle. Taken together, we suggest that the volume-sensitive anion channel, leading to RVD and taurine transport, is important for G1/S checkpoint progression in human cervical cancer cells.

The present study also showed that cell swelling induced both Cl^--dependent and -independent K^+ ($^{86}Rb^+$) efflux, presumably mediated by KCC and Ca^{2+}-activated K^+ channels, respectively. The KCCs of human cervical cancer cells is nearly quiescent under normal physiological conditions, but works synergistically with Ca^{2+}-activated K^+ channels for volume regulation in response to hypotonic stress. We have identified previously messenger ribonucleic acid (mRNA) transcripts of KCC1, KCC3 and KCC4 by reverse transcription polymerase chain reaction (RT-PCR) in human cervical cancer cells and confirmed by digestion with specific restriction endonucleases [32]. In addition, the activation of volume-sensitive KCC in cervical cancer cells is modulated by a phosphorylation cascade [32].

The role of Ca^{2+} in volume regulation of cervical cancer cells has been investigated in our previous study [6]. The activation of a volume-sensitive Cl^- channel requires the presence of extracellular Ca^{2+}. The time course of RVD is sensitive to both Ca^{2+} influx and discharge of intracellular stores. Here we demonstrated further that cell swelling induces K^+ transport via K^+ channels as well KCC. The activation of a volume-sensitive K^+ channel in cervical cancer cells depends on both extracellular Ca^{2+} influx and intracellular Ca^{2+} stores. In

contrast, the activation of volume-sensitive KCC, at least, is independent of extracellular Ca^{2+}. Volume-sensitive K^+ channels have been described in Ehrlich ascites tumour cells [7], tracheal epithelial cells [3], distal nephron A6 cells [21], bovine aortic endothelial cells [26], human T lymphocytes [12] and murine erythroleukaemia cells [35]. The relationship between Ca^{2+} and volume-sensitive K^+ channels is, however, controversial. For example, the activation of volume-sensitive K^+ channels depends on Ca^{2+} in Ehrlich ascites tumour cells [7], murine erythroleukaemia cells [35], MDCK cells [38] and human T lymphocytes [12]. On the other hand, swelling-activated K^+ efflux is not mediated by a Ca^{2+}-sensitive K^+ channel in bovine aortic endothelial cells [26] and cerebellar granular neurons [19].

The present study showed that the activation of swelling-activated K^+ efflux was independent of the cell cycle progression. This indicates that KCC and Ca^{2+}-activated K^+ channels have no association with the cell cycle clock of human cervical cancer cells, but we cannot rule out the possibility that other types of K^+ channel are involved in the regulation of the cell cycle in human cervical cancer cells. Indeed, expression of some types of K^+ channels correlates with the cell cycle clock. For example, the delayed-rectifier K^+ channel in lymphocytes is critical for cell cycle progression from G0 to G1, a transition which relies on membrane depolarization and requires a transmembrane flux of Ca^{2+} [27]. In mouse oocytes, a voltage-activated K^+ channel with a large conductance (241 pS) is active in the G1 and M phases but is inactive during the G1/S transition [9]. Arrest of spinal cord astrocytes at defined stages of the cell cycle clock also causes significant changes in the expression of voltage-gated K^+ currents [18]. Blockade of voltage-activated K^+ channels decreases proliferation of melanoma cells [20] and several types of neurons [24]. For MCF-7 human breast cancer cells, an adenosine 5′-triphosphate (ATP)-sensitive K^+ current is required for progression through G1 phase [15] and blockade of this type of K^+ channel causes MCF-7 cells to arrest in the Go/G1 phase [40]. Cl^- channels have also been implicated in the proliferative response of particular cell types. For example, the activity of the volume-sensitive Cl^- channel is down-regulated when muscle cells switch from a proliferating to a non-proliferative, differentiated state [37]. Alterations in the activities of volume-sensitive Cl^- channels have also been reported in the proliferative response of endothelial cells [36]. In human lymphocytes, permeability to Cl^- varies with the cell cycle stage, being low in G0 and S phases and increased in G1/S [2]. The expression of a glioma-specific Cl^- channel depends on the cell cycle stage and could be linked with cytoskeletal changes [34]. Although the exact role that ion channel activity plays in cell cycle progression is still ill-defined, changes in channel activity may result in both short-term modulation of pre-existing channel proteins and long-term changes in gene expression [27]. Other possible mechanisms for the involvement of ion channels in cell proliferation include transduction of mitogen-stimulated protein synthesis [39], rearrangements of cytoskeleton [31], generation of Ca^{2+} signals [8] and pH regulation [24].

In conclusion, this study provides new and important information on the functional significance of swelling-activated transport system in the regulation of cell cycle clock of human cervical cancer cells.

Acknowledgements This work was partly supported by the Wellcome Trust and National Science Council, Taiwan (NSC 89-2314-B-006-066 and NSC 90-2314-B-006-025). Meng-Ru Shen holds a Swire Scholarship supported by John Swire and Sons Ltd.

References

1. Alberts B, Bray D, Lewis J, Raff M, Roberts K, Watson JD (1994) Molecular biology of the cell 3rd edn. Garland, New York, pp 863–910
2. Bubien JK, Kirk LK, Rado TA, Frizzell RA (1990) Cell cycle dependence of chloride permeability in normal and cystic fibrosis lymphocytes. Science 248:1416–1419
3. Butt AG, Clapp WL, Frizzell RA (1990) Potassium conductances in tracheal epithelium activated by secretion and cell swelling. Am J Physiol 258:C630–C638
4. Chou CY, Shen MR, Wu SN (1995) Volume-sensitive chloride channels associated with human cervical carcinogenesis. Cancer Res 55:6077–6083
5. Chou CY, Shen MR, Chen TM, Huang KE (1997) Volume-activated taurine transport is differentially activated in human cervical cancer HT-3 cells, but not activated in HPV-immortalized Z 183A and normal cervical epithelial cells. Clin Exp Pharmacol Physiol 24:935–939
6. Chou CY, Shen MR, Hsu KS, Huang HY, Lin HC (1998) Involvement of PKC-α in regulatory volume decrease responses and activation of volume-sensitive chloride channels in human cervical cancer HT-3 cells. J Physiol (Lond) 512:435–448
7. Christensen O, Hoffmann EK (1992) Cell swelling activates K^+ and Cl^- channels as well as nonselective, stretch-activated cation channels in Ehrlich ascites tumor cells. J Membr Biol 129:13–36
8. Cornell-Bell AH, Finkbeiner SM, Cooper MS, Smith SJ (1990) Glutamate induced calcium waves in cultured astrocytes: long-range glial signaling. Science 247:470–473
9. Day ML, Pickering SJ, Johnson MH, Cook DI (1993) Cell-cycle control of a large-conductance K^+ channel in mouse early embryos. Nature 365:560–562
10. Hall JA, Kirk J, Potts JR, Rae C, Kirk K (1996) Anion channel blockers inhibit swelling-activated anion, cation, and nonelectrolyte transport in HeLa cells. Am J Physiol 271:C579–C588
11. Hoffmann EK, Dunham PB (1995) Membrane mechanisms and intracellular signalling in cell volume regulation. Int Rev Cytol 161:173–262
12. Khanna R, Chang MC, Joiner WJ, Kaczmarek LK, Schlichter LC (1999) hSK4/hIK1, a calmodulin-binding KCa channel in human T lymphocytes. Roles in proliferation and volume regulation. J Biol Chem 274:14838–14849.
13. Kirk K, Ellory JC, Young JD (1992) Transport of organic substrates via a volume-activated channel. J Biol Chem 267: 23475–23478
14. Kirk K (1997) Swelling-activated organic osmolyte channels. J Membr Biol 158:1–16
15. Klimatcheva E, Wonderlin WF (1999) An ATP-sensitive K(+) current that regulates progression through early G1 phase of the cell cycle in MCF-7 human breast cancer cells. J Membr Biol 171:35–46
16. Lang F, Busch GL, Ritter M, Volkl H, Waldegger S, Gulbins E, Haussinger D (1998) Functional significance of cell volume regulatory mechanisms. Physiol Rev 78:247–306

17. Levenson V, Hamlin JL (1993) A general protocol for evaluating the specific effects of DNA replication inhibitors. Nucleic Acids Res 21:3997–4004
18. Mac Farlane SN, Sontheimer H (2000) Changes in ion channel expression accompany cell cycle progression of spinal chord astrocytes. Glia 30:39–48
19. Morales-Mulia S, Ordaz B, Quesada O, Pasantes-Morales H (1998) Ca^{2+} changes and ^{86}Rb efflux activated by hyposmolarity in cerebellar granule neurons. J Neurosci Res 53:626–635
20. Nilius B, Wohlrab W (1992) Potassium channels and regulation of proliferation of human melanoma cells. J Physiol (Lond) 445:537–548
21. Nilius B, Sehrer J, De Smet P, Van Driessche W, Droogmans G (1995) Volume regulation in a toad epithelial cell line: role of coactivation of K^+ and Cl^- channels. J Physiol (Lond) 487: 367–378
22. Nilius B, Eggermont J, Voets T, Droogmans G (1996) Volume-activated Cl^- channels. Gen Pharmacol 27:1131–1140
23. Okada Y (1997) Volume expansion-sensing outward-rectifier Cl^- channel: fresh start to the molecular identity and volume sensor. Am J Physiol 273:C755–C789
24. Pappas CA, Ullrich N, Sontheimer H (1994) Reduction of glial proliferation by K^+ channel blockers is mediated by changes in pHi. Neuroreport 6:193–196
25. Parkin DM, Pisani P, Ferlay J (1993) Estimates of the worldwide incidence of eighteen major cancers in 1985. Int J Cancer 54:594–606
26. Perry PB, O'Neill WC (1994) Swelling-activated K^+ fluxes in vascular endothelial cells: role of intracellular Ca^{2+}. Am J Physiol 267:C1535–C1542
27. Premack BA, Gardner A (1991) Role of ion channels in lymphocytes. J Clin Immunol 11:225–238
28. Sakai H, Nakamura F, Kuno M (1999) Synergetic activation of outwardly rectifying Cl^- currents by hypotonic stress and external Ca^{2+} in murine osteoclasts. J Physiol (Lond) 515:157–168
29. Shen MR, Wu SN, Chou CY (1996) Volume-sensitive chloride channels in the primary culture cells of human cervical carcinoma. Biochim Biophys Acta 1315:138–144
30. Shen MR, Chou CY, Wu ML, Huang KE (1998) Differential osmosensing signalling pathways and G-protein involvement in human cervical cells with different tumor potential. Cell Signal 10:113–120
31. Shen MR, Chou CY, Hsu KF, Hsu KS, Wu ML (1999) Modulation of volume-sensitive Cl^- channel and cell volume by actin filaments and microtubules in human cervical cancer HT-3 cells. Acta Physiol Scand 167:215–225
32. Shen MR, Chou CY, Ellory JC (2000) Volume-sensitive KCl cotransport associated with human cervical carcinogenesis. Pflügers Arch 440:751–760
33. Shen MR, Droogmans G, Eggermont J, Voets T, Ellory JC, Nilius B (2000) Differential expression of the volume-regulated anion channel during the cell cycle progression of human cervical cancer cells. J Physiol (Lond) 528 (in press)
34. Ullrich N, Sontheimer H (1997) Cell cycle-dependent expression of a glioma-specific chloride current: proposed link to cytoskeletal changes. Am J Physiol 273:C1290–C1297
35. Vandorpe DH, Shmukler BE, Jiang L, Lim B, Maylie J, Adelman JP, de Franceschi L, Cappellini MD, Brugnara C, Alper SL (1998) cDNA cloning and functional characterization of the mouse Ca^{2+}-gated K^+ channel, mIK1. Roles in regulatory volume decrease and erythroid differentiation. J Biol Chem 273:21542–21553
36. Voets T, Szücs G, Droogmans G, Nilius B (1995) Blockers of volume-activated Cl^- currents inhibit endothelial cell proliferation. Pflügers Arch 431:132–134
37. Voets T, Wei L, De Smet P, Van Driessche W, Eggermont J, Droogmans G, Nilius B (1997) Downregulation of volume-activated Cl^- currents during muscle differentiation. Am J Physiol 272:C667–C674
38. Weiss H, Lang F (1992) Ion channels activated by swelling of Madin-Darby canine kidney (MDCK) cells. J Membr Biol 126:109–114
39. Wonderlin WF, Strobl JS (1996). Potassium channels, proliferation and G1 progression. J Membr Biol 154:91–107
40. Woodfork KA, Wonderlin WF, Peterson VA, Strobl SJ (1995) Inhibition of ATP-sensitive potassium channels causes reversible cell-cycle arrest of human breast cancer cells in tissue culture. J Cell Physiol 162:163–171
41. Zur Hausen H (1991) Human papillomavirus in the pathogenesis of anogenital cancer. Virology 184:9–13